

Contrasts in the coercivities of SmCo_5 and $\text{Sm}_2\text{Co}_{17}$ -type permanent magnets

H. A. Leupold, F. Rothwarf, J. T. Breslin, J. J. Winter, A. Tauber, and D. I. Paul¹⁾

U.S. Army Electronics Technology and Devices Laboratory (ERADCOM), Fort Monmouth, New Jersey 07703

We have extracted the intrinsic coercivity, saturation magnetization, and anisotropy field from M-H loop measurements in the TDK $\text{Sm}_2(\text{Co}, \text{Fe}, \text{Cu}, \text{Zr})_{17}$ and the Hitachi SmCo_5 permanent magnetic materials from liquid helium to room temperature. The TDK sample exhibits a coercivity in the hard direction which is larger than in the easy direction, while the reverse situation is true for the SmCo_5 sample. This behavior is linked to the difference in the mechanisms of magnetization dominating the sample, wall domain motion for the TDK sample, and domain nucleation for the SmCo_5 .

PACS numbers: 75.60. — d, 75.50.Cc, 75.30.Gw

INTRODUCTION

The increasing utilization of the SmCo_5 -type permanent magnets in microwave/millimeter wave tubes is due to their good saturation magnetizations coupled with extraordinarily high coercivities. The $\text{Sm}_2\text{Co}_{17}$ -type magnets, though displaying smaller but, for many purposes, adequate coercivities, have even higher saturation magnetization than the SmCo_5 types, thus affording the possibility of greatly increased energy products, $(BH)_{\text{max}}$. Because of extensive current use of such materials in microwave devices where temperature stability is of great importance, it is of interest to compare the temperature dependences of the magnetic properties of their commercial or proposed commercial forms. Accordingly, we have investigated a cube-shaped sample from TDK Company, Japan with a nominal composition $\text{Sm}_2\text{Co}_{10.3}\text{Fe}_{3.13}\text{Zr}_{0.194}\text{Cu}_{1.48}$ and a ratio of total transition metal to samarium content of $Z = 7.4$ and a second cube of composition SmCo_5 furnished by Hitachi. Microscopic observations of the former type of material indicate the presence of a copper-concentrated second phase precipitate which comprises the boundaries of a 500 \AA cellular structure (1) with domain wall pinning as the dominant dynamic mechanism of coercivity. In contrast, the coercivity of the SmCo_5 material is presumed to be primarily nucleation-controlled (2).

EXPERIMENTAL RESULTS

We have made M-H loop measurements in both the hard ($\theta = 90^\circ$) and easy ($\theta = 0^\circ$) magnetic directions of these materials from liquid helium to room temperature with an integrating fluxmeter and a superconducting magnet capable of providing fields up to 100 kOe. From these measurements we have extracted the temperature dependences of intrinsic coercivity, anisotropy field and saturation magnetization.

These quantities are displayed for the TDK samples in Figures 1a, 2a and 3a, respectively, and for the Hitachi SmCo_5 material in Figures 1b, 2b and 3b.

Figure 1a shows that for the TDK material the coercivity in the hard direction is greater than that in the easy direction over the entire temperature range measured, with maximum values at 0K of 17 and 15kOe, respectively. For SmCo_5 , the relationship of the coercivities in the hard and easy directions is reversed, with 0K values of 36 and 43kOe, respectively. We note that the curves in Figure 1a can be fitted by expressions of the form

$$H_c = \ln A \exp(-k_B T/E_1) + A_2 \exp(-k_B T/E_2). \quad (1)$$

Values for the A's and E's are tabulated in Table I.

TABLE I. Parameters for linear portions of coercivity curves.

Segment	Slope (Oe/K)	$\ln A_1$ (kOe)	E_1 (ergs) $\times 10^{-16}$
Easy TDK, $T < 60\text{K}$	-81.0	15.50	0.017
Easy TDK, $T > 100\text{K}$	-13.5	10.46	0.102
Hard TDK, $T < 150\text{K}$	-26.4	17.50	0.052
Hard TDK, $T > 150\text{K}$	-33.4	18.70	0.041
Easy SmCo_5 , $T < 60\text{K}$	-28.2	43.0	0.049
Easy SmCo_5 , $T > 120\text{K}$	-63.2	46.15	0.022
Hard SmCo_5 , $T < 100\text{K}$	-96.0	38.00	0.014
Hard SmCo_5 , $T > 200\text{K}$	-87.0	47.8	0.016

The SmCo_5 Hitachi sample shows an intrinsic coercivity in the easy direction of magnetization of the form of expression (1), decreasing from 43.1 kOe at 0K to 27.2kOe at 300K. For the hard direction, the curve also shows two regions of linear decrease in coercivity with temperature but with an anomalous peak of 32kOe between them at about 175K.

The anisotropy fields are defined as the values of applied field H_A at which the M-H curves for the hard and easy directions converge. Because the measured H_A are higher than our maximum applied field of 100kOe, extrapolation is necessary. The values thus obtained are then corrected by subtracting $4\pi M_s/3$, the demagnetization field for a sphere. Since this correction is less than three percent in all cases, the inaccuracy introduced by applying a spherical correction to a cube is negligible. Figure 2a shows that the anisotropy field of the TDK material decreases linearly from 166kOe at 4.2 to 115kOe at 300K with a slope of 0.186kOe/K.

Because of the larger extrapolations necessary to obtain the anisotropy fields for SmCo_5 , considerably more scatter appears in its H_A vs T curve than in that for the TDK specimen. (Compare Figures 2a and 2b.) Further, because of the regions of very high nucleation field known to be scattered throughout the SmCo_5 (2), the hysteresis loops are slightly skewed so that the extrapolated anisotropy fields are different for the first and third quadrants. Both sets of extrapolated data are constant with temperature to within the precision of the experiment, with an average value of $200\text{kOe} \pm 20\text{kOe}$.

The saturation magnetization ($4\pi M_s$) of the TDK specimen decreases monotonically from 10.8 kG at absolute zero to 10.2 kG at room temperature, while that of the SmCo_5 remains relatively constant (8.8 kG at 0K) up to about 250K beyond which it falls to 8.6 kG at 300K. (See Figures 3a and 3b.)

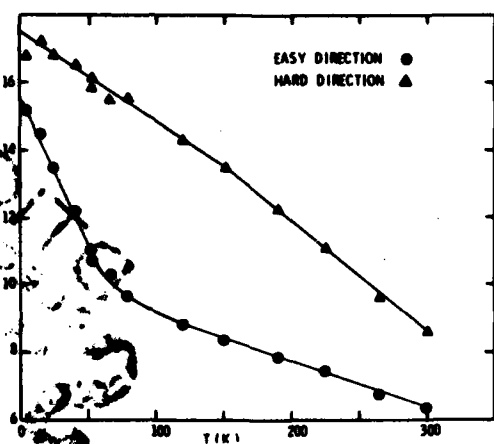


Figure 1a. Intrinsic coercivity vs temperature for $\text{Sm}_2\text{Co}_{10.3}\text{Cu}_{1.48}\text{Fe}_{3.13}\text{Zr}_{0.194}$.

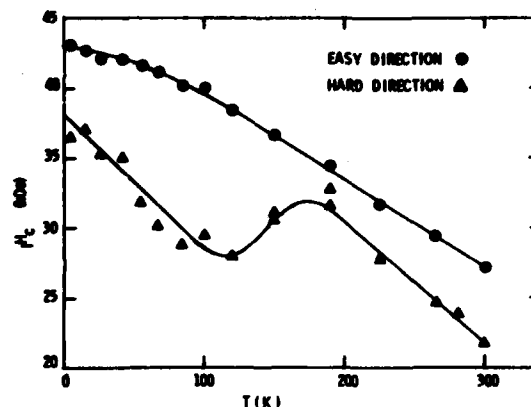


Figure 1b. Intrinsic coercivity vs temperature for SmCo_5 .

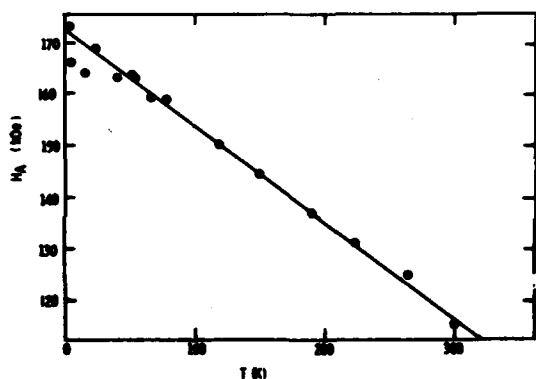


Figure 2a. Anisotropy field vs temperature of $\text{Sm}_2\text{Co}_{10.3}\text{Cu}_{1.48}\text{Fe}_{3.13}\text{Zr}_{0.194}$.

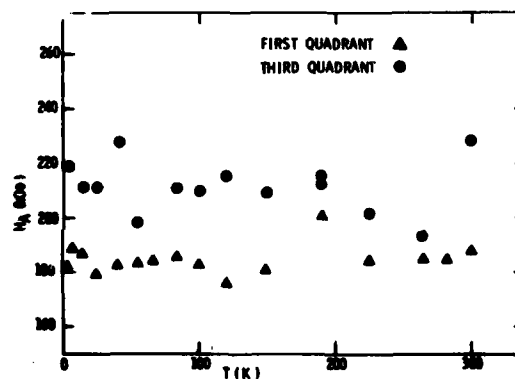


Figure 2b. Anisotropy field vs temperature for SmCo_5 .

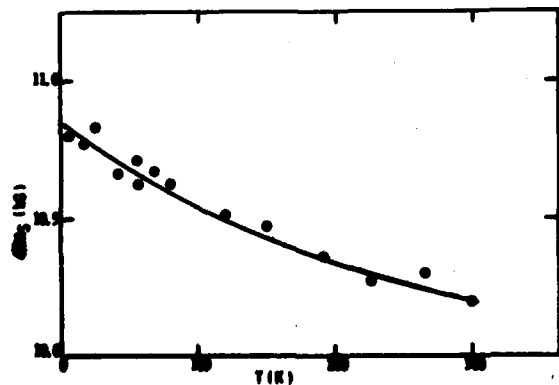


Figure 3a. Saturation magnetization vs temperature for $\text{Sm}_2\text{Co}_{10.3}\text{Cu}_{1.48}\text{Fe}_{3.13}\text{Zr}_{0.194}$.

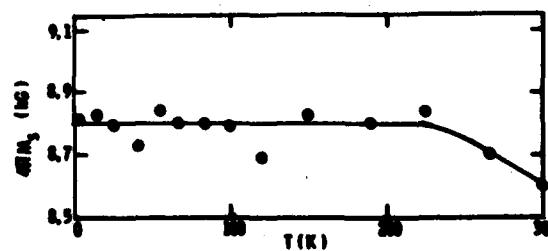


Figure 3b. Saturation magnetization vs temperature for SmCo_5 .

DISCUSSION

The drop in coercive force with increasing temperature may be the result of two contributions: (1) the decrease of both anisotropy field and saturation magnetization with increasing temperature; (2) the increase in thermal vibrational energy of the ferromagnetic domain walls with rising temperature. For the TDK sample whose coercivity in the easy direction is controlled by domain wall pinning, the first contribution can be estimated with the formula for coercive force given by Paul (3).

$$H_C = \pm H_A^{3/2} (M_s/6A)^{1/2} W(\eta + \alpha)/3, \quad (2)$$

where A , W , η and α are assumed to be independent of T . Equation 2 is applicable to domain wall pinning by defects of narrow width W and small deviations from the host material in anisotropy η and exchange α . The quantities H_A and A are the bulk anisotropy field and exchange constant, respectively. We see from this expression that the contribution of the anisotropy field to the coercive force is in proportion to its $3/2$ power. Substitution of our experimental data for H_A and M_s into (2) yields an approximate value for $H_C(4.2K)/H_C(300)$ of 1.8, compared with the value of 2.4 observed experimentally. We are not, however, able to obtain a quantitative model for the change in slope at approximately 80K. One must also consider the effect of contribution (1) to the coercive force due to the reduced difficulty in nucleating domain walls with increasing temperature. For this we do not yet have any analytic expression. Contribution (2), the increase in thermal vibrational energy, was considered by Gaunt (3) who showed that the change in coercive force with temperature due to this mechanism can be written as

$$\Delta H_C = 25k_B T/MA'W, \quad (3)$$

where A' is the domain wall area. The magnitude of

ΔH_C in the formula is difficult to estimate without a knowledge of the other parameters. The formula does, however, predict a linear decline of coercive force with temperature and thus cannot account for the change in slope at $T = 80K$ unless one assumes a change in A' or W at that temperature. The other coercive force vs temperature graphs (i.e., TDK magnetized in the hard direction and $SmCo_5$ in either direction) reflect rotation and/or nucleation domination and we do not have any analytic expressions for them.

The higher H_C in the hard direction of the TDK material is as expected for a material in which domain wall pinning is the dominant coercivity mechanism. Indeed, a reciprocal $\cos \theta$ dependence results from several different pinning models (5,6,7) for such systems, most notably that of Kondorsky (5).

The case of nucleation controlled coercivity, as in $SmCo_5$, is somewhat more complex. Here the relative magnitude of $H_C(0)$ and $H_C(90^\circ)$ depends upon the maximum magnetizing field H_M to which the sample has been subjected prior to and in the direction of the coercivity measurement. According to this model (2), if H_M is sufficiently high, that is of the order of a quarter or greater of the maximum observed coercivity, $H_C(0)$ will exceed $H_C(90^\circ)$. In our measurements H_M is close to 100kOe while the largest coercivity is only 43kOe. Thus, the condition for a larger easy direction coercivity is easily satisfied and is consistent with the experimental results.

REFERENCES

- a. Permanent address: School of Engineering, Columbia University, New York, NY 10027
1. T. Ojima, S. Tomezawa, T. Yoneyama, and T. Hori, IEEE Trans. Magn. MAG-13, 1317 (1977)
2. J. J. Becker, J. Appl. Phys. 38, 1015 (1967)
3. D. I. Paul, A.I.P. Conf. Proc. 29, 545 (1975)
4. P. Gaunt, J. Appl. Phys. 43, 637 (1972)
5. E. Kondorsky, J. Phys. USSR 2, 161 (1940)
6. J. Bernasconi, S. Strässler, and R. S. Perkins, A.I.P. Conf. Proc. 24, 761 (1979)
7. E. C. Stoner, and E. P. Wohlfarth, Phil. Trans. Roy. Soc., London A240, 599 (1948)

Accession For	
NTIS GRA&I	<input checked="" type="checkbox"/>
DTIC TAB	<input type="checkbox"/>
Unannounced	<input type="checkbox"/>
Justification	
By _____	
Distribution/	
Availability Codes	
Dist	Avail and/or Special
A	21